

DESIGN, SIZING AND OPTIMIZATION OF A SOLAR- WIND HYBRID POWER SYSTEM

ABSTRACT

Design, sizing and optimization of a solar-wind hybrid power system was carried out to determine its economic feasibility using Hybrid optimized model for electric renewable (HOMER) software aimed at selecting the most feasible configuration based on the net present cost to meet the load demand of 425 W for the appliances in a departmental office at Joseph Sarwuan Tarka University, Makurdi. The simulation results were used to develop a working prototype by sizing the four major components: the solar panels (350 W), a wind turbine (100 W), 2 battery systems of 12 V/200Ah and a charge controller (35.4 A) to regulate battery charging. The efficiencies of the wind turbine, PV solar panels and the inverter system were 48, 29.2 and 50 % respectively. The contribution of PV was 98 % and that of the wind turbine was 2 % due to low average wind speed (1.96 m/s at 15 m) from February to April. The results showed that solar energy contributed more to the charging of the inverter than the wind energy due to the high favorable solar insolation in the region. The optimized system configuration was chosen and this was based on the net present cost, levelized cost of energy and its renewable fraction respectively. The results demonstrated that the best hybrid combination consists of 0.35 kW PV Panels, 1 unit of 0.1 kW wind turbine, 2 units of deep cycle batteries (12V each/200Ah) and 1 unit of 1600 W Inverter. The prototype of the solar - wind hybrid power system based on the optimized components met the load demand for the basic appliances in the office. The results can be expanded to cover the entire department and the templates so obtained can be used generally within the University Community.

Keywords: Inverter, Levelized energy cost, Optimization, Solar insolation, Solar-wind hybrid, wind turbine

INTRODUCTION

Increasing environmental awareness, conservation of natural resources, rising cost of fossil fuels and the continuous search for lowering energy dependency on fossil fuels, have motivated the development of national legislations enabling the deployment of alternative energy technologies [1, 2]. To improve a nation's energy independence and security, the best solution is to efficiently use renewable energy resources including solar, wind, hydro, geothermal, and tidal energy [3].

Hybrid power systems consist of a combination of renewable energy sources. It may comprise of components such as solar panel, wind turbine, batteries, inverter and charge controller which can be connected in different architectures. This energy sources are used in conjunction with energy storage equipment (batteries). This is often done either to reduce the cost of generating electricity from fossil fuels or to provide back up for renewable energy systems, ensuring continuity of power supply [4, 5].

In order to optimize the use of the renewable energy sources, wide-scale distributed renewable energy systems (DRES) are more widespread than the large-scale centralized installations [6]. The environment could be protected from further deterioration if the renewable energy sources are used more intensively for the production of energy. Furthermore, solar and wind energy are free and clean and although available at variable levels related to the local environmental parameters (insolation, wind speed and temperature), their long life-time and low maintenance requirements make them attractive [7]. As shown by [8], the combinations of photovoltaic and wind turbine systems with energy storage source to respond to the lack of power under load peaks, have a widespread use, to insure a continuous and reliable energy source for consumers. Shaffic *et al.* [9] considered the integration of solar and wind energy as a hybrid energy generation system mainly focusing on sizing and optimization. Other studies centered on the energy management system designed on minimizing the micro grid operating costs or maximizing the revenues according to the distributed generation bids and the market price of energy [9].

Much work is has been done in this area, with opportunity for more. Reddy [10] carried out a review which focuses on four essential categories of hybrid renewable energy systems which are sizing (using software or traditional methods), optimization (classical, artificial and hybrid methods), control (centralized, distributed and hybrid control) and energy management (technical objective, economic objective and techno-economic objective). Furthermore, the paper compared between different methods used in each category.

Hadi *et al.* [11] carried out the sizing and economic analysis of a stand-alone hybrid photovoltaic-wind system for rural electrification with Lundu Sarawak as a case study. The aim was to obtain an optimization of a hybrid PV-wind system in terms of sizing and cost over a 20 years period. The system simulation was done in MATLAB for

verification. It included a detailed computation using a life cycle cost method to identify all possible combinations. The optimal combination had 11 solar panels, one wind turbine and 9 batteries. A sensitivity test of the results verified by the simulation identified the most deterministic system affecting the life cycle cost of the system. Finally, total cost distribution of the optimized system showed that 50% system cost was contributed by the wind turbine. The determination of the life cycle cost was done as a combination of component and operation costs, and it was identified that replacement cost had the highest contribution while the wind turbine had the highest operation cost from the system cost.

Weiping *et al.* [12] proposed a new hybrid optimization algorithm for the optimal sizing of a stand-alone hybrid solar and wind energy system based on three algorithms: chaotic search, harmony search and simulated annealing. To improve the accuracy of the size optimization algorithm results, weather forecasting was used along with artificial neural networks for solar radiation, ambient temperature, and wind speed forecasting. The main objective function of minimizing the total life cycle cost was used to assess the feasibility of the hybrid renewable energy system accounting for system reliability. The reliability of the system was assessed by the loss of power supply probability parameter. The new method was tested for the electrical load of the city of Khorasan, Iran. The results were compared with those obtained by the proposed algorithm (harmony search and simulated annealing-based artificial neural networks). The simulation results demonstrated the advantages of utilizing the hybrid optimization algorithm with weather forecasting data for a stand-alone hybrid renewable energy system.

Environmental concerns deriving from the use of fossil fuels has necessitated the urgent need for the utilization of renewable energy resources for power generation. Global warming have consequences recognized as significant risks to civilization, while climate change resulting from the burning of fossil fuels is occurring faster than as estimated by scientists [13]. Hybrid solar and wind energy ranks high among renewable sources as a promising solution to provide reliable power more efficiently with reduced requirements for stand-alone applications. Furthermore, the finite supply and environmental costs of using fossil fuels has created the great need for renewable energy sources. In order to meet growing demands for energy, there is a need to exploit all sources, with renewable sources being unlimited and clean though often intermittent. To overcome this problem, several energy sources are combined to obtain a hybrid renewable system. Hence, designing, sizing and optimizing a hybrid renewable energy system is imperative.

The aim of this research is to design, size and optimize a solar - wind hybrid power system capable of powering some the appliances in the office of the Head of Department Mechanical Engineering, Joseph Sarwuan University, Makurdi, Nigeria. The specific objectives were the evaluation of the consumption pattern of the appliances in the office and determination of the feasibility of using such a system as an alternative, as well as the design, sizing and optimizing the solar-wind hybrid power system that could be expanded for further applications. The environmental hazards derived from the utilization of fossil fuel resources has necessitated an urgent need for renewable energy sources. The study provides an environmentally clean renewable energy source and also provides a hybrid power generating system that is reliable and economical to run.

Theoretical Background

The design, sizing and selection of a solar-wind hybrid system is done using standard methods. To develop the power system, performance investigation, modelling and mathematical calculations have to be carried out [14]. Different models of hybrid system have been covered in various literatures. The components required include meteorological data, load demand and system configuration.

Meteorological analysis of the location has to be made for the optimization process. It is important for total utilization of PV/wind sources. Measuring solar and wind resources data are the main input of the hybrid system [15]. Load demand is very significant in the design and sizing of a solar-wind hybrid power system. Load variation for different seasons is not predictable, therefore the solar- wind hybrid power system has to be designed for nearer or more than load demand to fulfil the requirements [16]. By studying all the data like solar radiation, wind speed and load demand, proper selection of equipment have to be made. However, sizing of the system will be according to the environmental conditions because producing power from solar-wind hybrid power system depends upon the location selected [17].

There are six basic steps involved in the design and planning of a hybrid system which are evaluation of meteorological conditions, analysis of electric load demand, hybrid system configurations, hybrid system model development, analysis using simulation and optimization, and operational analysis of resulting system. The first step is to estimate the average power demand of each load to be used for the location [18, 19]. The average load capacity can be computed using equation 1.

$$\text{Average Load Capacity (Wh)} = \frac{\text{Total Estimated Load}}{\text{Operational hours}} \quad (1)$$

The operational hours during the day gives a more accurate sizing of the solar-wind hybrid power system that will be needed to power the appliances under consideration [15]. Due to the fact that solar and wind resources in a location are intermittent and unpredictable in nature, integrating the two renewable resources into an optimum combination the impact of the variable nature of the resources can become more reliable and economical to run [20]. Cost is an important economical factor in selecting or developing a hybrid system. The sub criteria to be used in the preliminary evaluation of cost are capital cost, fuel cost and operations and maintenance cost. For a solar - wind hybrid power system to be feasible it must be cost competitive [6].

The design process of hybrid energy systems requires the selection and sizing of the most suitable combination of energy sources, power conditioning devices and energy storage system together with the implementation of an efficient energy dispatch strategy [21]. The selection of the suitable combination from renewable technology to form a hybrid energy system depends on the availability of renewable sources. Other factors that may be taken into account for proper design depends on the load requirements such as reliability, greenhouse gas emissions during the expected life cycle of the system, efficiency of energy conversion, land requirements, economic aspects and social impacts [22, 23]. The unit sizing and optimization of a hybrid power system plays an important role in deciding the reliability and economy of the system.

For a given hybrid energy system, the design stage facilitates the determination of the type of renewable energy system to be included, number and capacity of renewable energy units to be installed, energy storage that would be integrated into the system, and whether the system is stand-alone or grid-connected. The selection of the technology depends on the availability of renewable resources for the particular site where the system is to be installed. Based on the weather statistics (hourly data), a feasibility study for different possible combinations of renewable sources is studied using optimization techniques to get the optimum configuration and then the number and size of the selected components is optimized in order to get an economical, efficient and reliable system. Oversizing of the components may lead to high system cost and therefore the system may become economically unviable. On the other hand, under-sizing will reduce the initial cost but one has to compromise system reliability. Recently, many more software packages such as HOMER and RETScreen have been developed for the proper selection of suitable generation technologies and their sizes. The packages have made the study of hybrid systems interesting and easier. Optimization-based approaches that simultaneously minimize the investment cost (installation and unit cost) and fuel cost while retaining the reliability and emission constraints have been implemented [24, 25]. The optimization criterion for hybrid energy systems includes economic aspects and technical variables.

For the economic aspect, the net present cost (NPC) is a summation of all costs: capital investment, non-fuel operation and maintenance costs, replacement costs and energy costs. If a number of options are being considered, the option with the lowest net present cost will be the most favourable financial option. Cost of energy (COE) is a calculation of the cost of generating electricity at the point of connection to a load or electricity grid [26].

The technical variables include supply reliability, battery throughput and environmental factors. An energy source is considered reliable on a site if it can be used to generate consistent electrical output and is available to meet predicted peak in demand. Battery throughput measures the performance and storage capacity of a battery that is used for a specific purpose. The environmental factors include renewable fraction, carbon dioxide emissions and site conditions [27].

After defining the criteria to be considered, the main optimization principle in the objective function might be as diverse as minimum cost, maximum financial viability, minimum carbon dioxide emissions, minimum investment and/or maintenance cost, minimum annual fuel cost, maximum continuity of supply, unmet load. The methodology for the design of hybrid renewable power systems depending on availability of energy sources and load characteristics is a primary point of concern [27, 28].

Solar-wind hybrid power system consists of wind turbine, photovoltaic array, charge controller and battery. Wind turbines convert wind energy into mechanical energy and then into electric energy. Whatever electric energy is generated from this system is alternate and unstable so some controlling units or inverters are used. This energy is utilized for domestic and residential purposes and this energy is in DC form [29].

Photovoltaic technology involves the direct conversion of sunlight into electricity through the use of PV modules. These solar cells are composed mainly of silicon. Under certain conditions, electrons from silicon atoms can be released and become available to move as part of an electric current. When solar cells are joined physically and electrically and placed in a frame, they form a solar panel or PV module. The basic building block of a photovoltaic module is the photovoltaic cell. These converts solar energy into electricity [30]. The power output will depend on the amount of energy incident on the surface of the cell and the operating temperature of the photovoltaic cell. The three currently dominating cell technologies are mono-crystalline, polycrystalline and thin film cells [28, 31]. The overall efficiency of the module depends on the cell efficiency, placement within the module and on the laminating materials used [32].

To determine the size of PV module, the required energy consumption must be estimated. Therefore, the PV module size can be determined using equation 2.

$$PV \text{ module size} = \frac{\text{Daily Energy Consumption}}{\text{Insolation} \times \text{Efficiency}} \quad (2)$$

Where insolation is in kWh/m²/day, the energy consumption is in Watts and efficiency of solar panel is given by equation 3.

$$\eta_{sp} = \frac{P_m}{E_m \times A_c} \quad (3)$$

Where P_m = maximum power output, A_c = Area of collector, E_m = Incident radiant heat flux (W/m²) = 1000 W/m². Also, the solar panel wattage can be estimated using equation 4.

$$\text{Solar Panel Wattage} = \frac{\text{Total Load (Wh)}}{\text{Operational hours}} \quad (4)$$

The quantity of power transferred to a wind turbine is directly proportional to the area swept out by the rotor to the density of the air and the cube of the wind speed. The power in the wind turbine (P_w) can be determined using equation 5.

$$P_w = \frac{1}{2} C_p \rho A V^3 \quad (5)$$

Where C_p = Power coefficient, ρ = Air density (kg/m³), V = Wind speed, A = Swept area of the wind turbine given by equation 6.

$$A = \frac{\pi D^2}{4} \quad (6)$$

Where D = Rotor blade diameter (m). Equation 6 can also be written as A = πl² from where the circumference of the turbine (C) = π D.

The tip speed ratio is given by equation 7.

$$\text{Tip Speed Ratio} = \frac{\text{Blade Speed}}{\text{Wind Speed}} \quad (7)$$

The efficiency of the wind turbine system can be determined using equation 8.

$$\eta_{WT} = \frac{\text{Actual Power output of wind turbine}}{\text{Power due to wind}} \quad (8)$$

The theoretical maximum power efficiency of any design of a wind turbine is 0.59 (i.e. not more than 59 % of the energy carried by the wind can be extracted by a wind turbine). This is called the “power coefficient” and is given by equation 9.

$$C_{p,max} = 0.59 \quad (9)$$

The C_{p,max} value is unique to each turbine type and is a function of wind speed that the turbine is operating in. Once the various engineering requirements of wind turbine are incorporated, specifically strength and durability in particular, the real world limit is well below the Betz Limit with values of 0.35-0.45 common even in the best designed wind turbines. By the time other factors are taken into account in a complete wind turbine system such as the gearbox, bearings, and generator, only 10-30 % of the power of the wind is actually converted into usable electricity.

The rotor is the most important component in a wind turbine designed to capture wind energy and convert it into rotating mechanical energy. Hence, the rotor should be strong enough to withstand periodic and randomly changing loads [33, 34]. The rotor assembly consists of several blades joined to a common hub, a cone nose and fasteners. The blade is a critical component of the rotor and consists of the air foils which interact with the wind and convert the power in the wind to mechanical power. The geometry and dimensions of the blades are determined by the performance requirements of the wind turbine. Two fundamental issues must be considered simultaneously in blade design process: aerodynamic performance and structural design [35]. Aerodynamically advantageous features such as sharp trailing edges are often difficult to build. Compromises must be made so that the designed blade can be manufactured, and the choice of materials and manufacturing methods for the blades should also be considered during structural design and strength analysis [36, 37]. The hub is the part which transmits all the power and load from the blades to the main shaft. There are three types of hubs: rigid, teetering and hinged hubs [33]. A rigid hub is the simplest and most common, and it supports the blades in fixed position relative to the main shaft.

In all electricity generating wind turbines, a generator converts the mechanical power from the rotating wind blades to electrical power. Induction and synchronous generators are among the most common generators in large wind turbines [28]. Most small wind turbines use direct drive generators which are actually special synchronous generators with enough poles to enable the generator work well at the same speed of the rotor [38], and because

there is no gear box required with this generator, the reliability of the system is generally better than when a gear box is included [39]. The nacelle houses all the principal components of the wind turbine except the rotor. Within the nacelle a main frame provides the backbone of the wind turbine which include the bearing supporting the hub, generator, tail assembly and yaw bearing are all connected to it. A nacelle cover protects these components from weather elements [32].

Most small wind turbines are pointed into the wind using a tail assembly. A tail assembly usually consists of tail fin and tail boom which are the primary components of the yaw system keeping the turbine pointed into the wind. Larger turbines generally dispense with a tail because as the turbine size increases the weight and loads associated with a tail become excessive. Instead most large turbines use an active yaw system in which geared motors point the turbine into the wind based on the readings of wind direction sensors mounted on the nacelle. In many small wind turbines, the tail assembly includes an auto-furling system. Furling occurs if the thrust becomes too great and the rotor pivots relative to the tail fin, which is hinged where it joins the main frame, with the effect of turning the rotor to face away from the prevailing wind direction [7]. When wind speed is below the rated critical value, the rotor is kept oriented to the wind; otherwise, furling will work to protect the rotor and generator.

Batteries are used to store energy in stand-alone applications for use at times when no insolation is available (e.g. night, rainy day). They are also used for diverse number of applications including standby power and utility interactive schemes [40]. The batteries in use for the hybrid system are storage batteries meant to provide backup and when the solar radiation is low especially in the night hours and cloudy weather. The battery to be used must be able to withstand several charge and discharge cycles, and operate within the specified limits. Batteries require tolerance to deep discharges and irregular charging patterns. Some applications may require the batteries to remain at a random state of charge for prolonged time. Their capacities are dependent on several factors which include age and temperature. Batteries are rated in ampere-hour (Ah) and the sizing depends on the required energy consumption. If the average value of the battery is known and the average energy consumption per hour is determined the battery capacity is determined by equations 10 and 11.

$$BC = \frac{2 \times f \times w}{V_{Battery}} \quad (10)$$

Where BC = Battery capacity, f = Factor for reserve, w = Daily energy, $V_{battery}$ = Battery voltage.

$$Ah \text{ rating} = \frac{\text{Daily Energy Consumption}}{\text{Battery rating at a specified voltage}} \quad (11)$$

The energy stored in a battery in kWh is given by equation 12.

$$\text{Energy Stored} = \frac{Ah \times V_{Batt}}{1000} \quad (12)$$

Where V_{batt} = Battery voltage and Ah = Ampere hour rating.

Batteries are available in two major categories which are flooded (vented) and valve regulated batteries. The amount of energy a deep cycle battery can store is referred to as its capacity. The unit that describes capacity is the Amp-hour (Ah). Often batteries will appear to have multiple ratings due to this rating process [37]. The three charging stages of a battery are boost, floating and trickle stages. The boost stage is identified when the battery needs to be charged or after being drained off while supplying the D.C load as well. The floating stage is identified when the battery is always in a charged condition. As the batteries keep draining at this stage, the float charger will again increase the charging voltage and the charging process continues. At this stage charging is done for a long period of time and its purpose is to keep a battery from draining. The trickle stage is identified when the battery is charged at a fully charged rate equal to its self-discharge rate, thus enabling the battery to remain at its fully charged level. Battery is charged to make up for the internal battery losses and this keeps battery charged to its full level [24, 32].

An inverter is a device that converts DC power from the battery bank to AC power for various loads. In larger systems incorporating components that demand AC power, an inverter must be utilized [41]. Also, if the instrument site is located some distance from the power production site, an inverter allows for an efficient means of getting electricity to the point of use. The size of an inverter is computed using equation 13 [21].

$$\text{Total load} + (50\% \times \text{Total load}) \quad (13)$$

The efficiency of the inverter is calculated using equation 14.

$$\eta_{Inv} = \frac{\text{Average onload voltage}}{\text{Average of flaad voltage}} \quad (14)$$

Two fundamental categories of inverters are synchronous and static or stand-alone. Synchronous inverters are capable of being tied into the electrical grid or utility power. Except in the largest of infrastructure-based systems, this type of inverter finds little application in the field of solar research. Static inverters are designed for independent, utility-free power systems and are the type most often used for remote PV applications [42].

A second inverter classification refers to the type of AC waveform they produce. Inverters are available in **square, modified square, and** sine wave outputs. The criteria to be considered when selecting an inverter are

- a. DC voltage input must match the battery voltage of the system.
- b. AC power output must be adequate to satisfy the maximum-potential combined AC load, or all of the AC-powered equipment that might be **in use** at one time.
- c. Voltage and frequency regulation should be very tight in a high-quality unit, **and should match** the system requirements [15, 27, 43].

A charge controller is a DC to DC converter whose main function is to control the current flow from the hybrid power system **for** charging batteries. A charge controller monitors the battery state of charge to ensure that when the battery needs charge **current, it is attended to** and also ensures **that the** battery is not overcharged [44, 45]. The charge controller current is determined using equation 15.

$$I = \frac{P}{V_{Battery}} \quad (15)$$

Where P = Load capacity, $V_{Battery}$ = Voltage of battery, I = Expected charging current [16, 46].

HOMER sizes up the system specifications such as the load profile, wind resources, solar resources, system control parameters and constraint parameters as well as components technical and economic details. It performs **a number** of hourly simulations to ensure the best possible matching between the load and the supply in order to design an optimal system. **Thereafter**, it creates a list of feasible system configurations, sorted according to cost effectiveness and presents the optimal configuration based on the net present cost (NPC) [39]. Climatic data (wind speed and solar insolation), site load profile, hybrid system components, technical details and cost, system control as well as system constraints serve as input to the software [47].

MATERIALS AND METHOD

The design and sizing of the solar- wind hybrid power system was done using standard methods **at the Department** Mechanical Engineering departmental office located at the ETF block of Joseph Sarwuan Tarka University, Makurdi which lies on Latitude $7^{\circ} 7' N$ and Longitude $8^{\circ} 5' E$. Sizing was done for all the hybrid components including the **load** capacity. The solar panels and the wind turbine were mounted and placed outside the departmental office to harvest available solar and wind. The inverter had two terminals for the solar and wind sub-systems **connections** respectively. The inverter had an AC outlet in which various loads were plugged for optimum use. The measurements of the electrical quantities were carried out using an AVD-830D digital multimeter.

The test appliances used include a desktop computer of 100 W, two fans of 65 W each, one laptop of 75 W and six energy bulbs of 20 W each. The offload **(no load) voltage** on the inverter had fluctuations within the range of 23.5 to 23.8 V when fully charged. Two batteries of 12 V each were connected in **series** to generate a 23.8 V effect. The loading consumption was estimated from the electrical appliances power rating needs as presented in Table 1. The load demand was approximately 2975 Wh and 425 W peak. The daily profile pattern obtained from the HOMER software (Homer Beta 2.0) is shown in Figure 1.

The photovoltaic module sizing was carried out **using** equation 4 based on the total load and load demand. Hence, solar panel of 425 W was needed for this design. For a solar panel of 175 W, the number of panels arranged in parallel to achieve 425 W was $425/175 = 2.4$. Hence, two AP-PM-175 solar panels were selected for the study [41].

According to [21], to make the chosen battery to last long it **was** assumed that only a quarter of the battery capacity will be made **used so** that it will not be over discharged. For the total load of 425 W, operational hour is 7 hours and total load demand is 2975 Wh, the required battery capacity was $2975 \times \frac{1}{4} = 744 Wh$. The choice of the battery hour depends on the ampere-hour rating of the storage battery. Therefore, for a 425 W, 12 V battery, the number of batteries needed was $744/425 = 1.75$. Therefore, two VLA6CRV220 batteries were used for the design. The current of the charge controller was estimated to be 35.4 A using equation 15.

The power in the wind hitting the wind turbine with the design swept area was estimated by employing equations 5 and 6 **respectively**, using the experimental average wind speed value for Makurdi region during the period of the study (1.96 m/s), the power in the wind hitting the wind turbine was estimated to be 118 W. The sizing of the inverter was carried out by employing equation 13. However, an inverter size of 1600 W (2 kVA) was used in **order** to prolong the life span of the inverter [48].

The solar insolation measurement was carried out using a TES 1333 solar power meter calibrated in W/m^2 from February to April. The device was placed 0.5 m above the ground with the sensor pointing in the direction of the sun. The meter was set on to measure the solar insolation intensity and the values were read from the screen at hourly intervals. The mean values of insolation were computed and recorded. Also, the daily wind speed for the

location was measured and recorded using an AM4812 fan anemometer for the same period. From the solar insolation and wind speed data collected, the annual average was determined.

Table 1. Load Consumption Pattern

Appliances	Quantity	Load (W)	Operational Time	Total Load (Wh)
Energy bulbs	6	20	9a.m – 4 p.m	840
Fans	2	65	9a.m – 4 p.m	910
Desktop computer	1	100	9a.m - 4 p.m	700
Laptop	1	75	9a.m – 4 p.m	525
TOTAL		425		2975

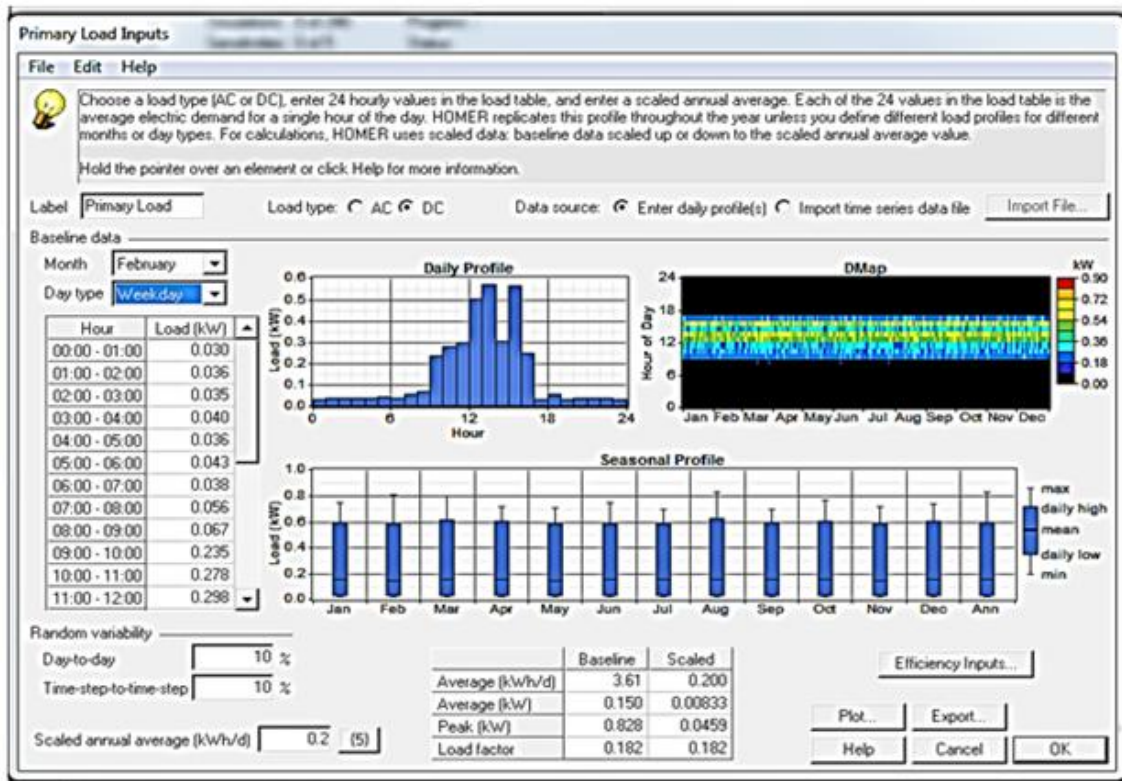


Fig. 1. Daily Profile pattern

The properties of materials, performance requirements, material reliability, safety, environmental conditions, availability and economic factors were considered in selecting the materials used for the fabrication of the inverter, wind generator and solar panel support stand. The permanent magnet generator (PMG) consists of components such as shaft, armature, magnet and electric copper coil. Permanent magnet generator is considered the best choice for small wind turbines because it rotates easily and requires low inertia to start producing electricity. The blade material selected for the wind turbine was Aluminium due to its light weight and easy workability [35, 48, 49].

For the design, two polycrystalline modules of 175 W solar panels were used. The panels were made of anodized aluminium alloy with the solar panel design specifications of the manufacturers strictly adhered to. Two deep cycle batteries of 12V each were used and connected in parallel. A charge controller was used and this controller serves to maintain the proper charging voltage on the batteries. The controller has one output for the battery bank and inputs for the solar panel and the wind turbine. Figure 2 shows the charge controller used in this research.



Fig. 2. The Charge Controller

A 6 mm flexible wire was used to connect the solar panel and the wind turbine to the inverter. There were two important connections in this system which were the connection from the wind turbine and solar panel to the charge controller and the connection from the charge controller to the input terminals of the battery.

In any off-grid energy system, it is important to select a shield frame to install the batteries, inverter and other electrical components. The shield frame must be protected from rain and other environmental conditions and should have proper ventilation. The material used for the shield frame fabrication was mild steel. The choice of this material was based on the cheapness, ease of machining and weldability. Figure 3 shows the inverter used.

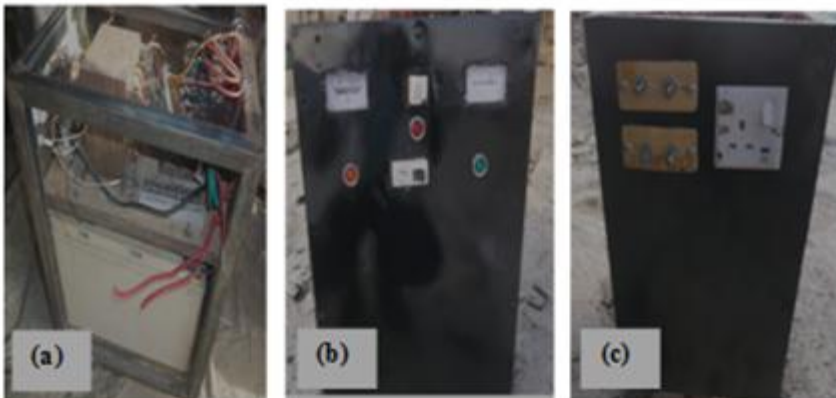


Fig. 3. The Inverter used: (a) Batteries connection, (b) Front view and (c) Rear view

A collapsible solar panel support frame was constructed using mild steel round pipe. The fabricated frames were measured based on the actual area ($1570 \times 680 \times 35$ m) of the solar panels used. They were fabricated such that the solar panel could be adjusted or properly positioned for maximum tracking of the sun. A 2 mm mild steel angle iron was used to provide placement for the installation of the solar panels while the two inches round mild steel pipe was used specifically for the fabrication of the solar panel support stand.

The wind turbine comprised of the permanent magnet generator which converts the kinetic energy in the air to electrical energy. A rectifier was installed for converting the direct current generated to alternating current. As the blade turns, kinetic energy is converted to electric energy. The wind turbine unit showing the PMG is shown in Figure 4. The diagram of the whole system is shown in Figure 5.

Testing was done with a focus to determine relevant parameters to ascertain the conformity of the system with the required standard conditions. The swept area of the turbine was determined by employing equation 6 given the length of the blade to be 0.8 m and the circumference of the turbine was determined from the expression $C = \pi D$ as earlier described. The swept area of the rotor and the circumference of the turbine were determined to be 2.01 m^2 and 5.02 m respectively.

The tip speed ratio of a blade is the ratio between the tangential speed of the tip of a blade and the actual velocity of the wind. The tip speed ratio was determined using equation 7. The blade speed was evaluated as the time taken for one turbine blade to achieve one complete revolution in relation to the circumference of the rotor. The time taken for the blade to make a complete revolution was 0.0167 min. Hence, blade speed = $5.02/0.0167 = 300.6 \text{ m/min}$. To convert the blade speed to mph, a factor of 0.0372 was used to multiply it [38]. Therefore, Blade speed = $300.6 \times 0.0372 = 11.18 \text{ mph}$. The experimental value of wind speed at the test location was determined to be 1.96 m/s. By employing equation 7, tip speed ratio = 2.54, implying that the turbine blade system is a slow running system with the ratio between 1 and 4 for a three blade system [38]. Figure 5 shows the general layout of the system.



Fig. 4. Wind Turbine Hub and Generator assembly

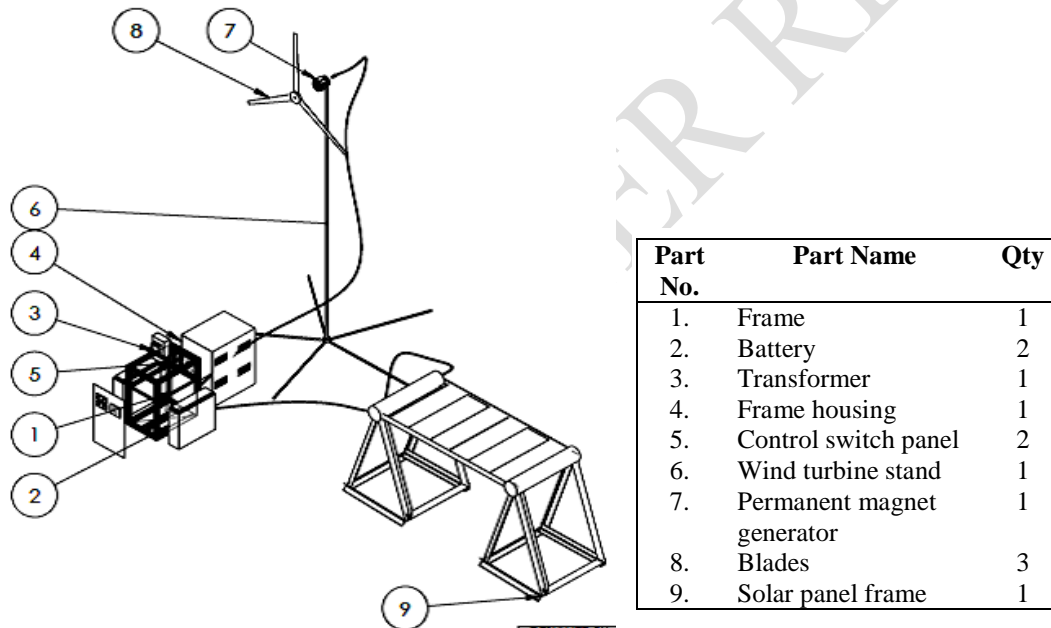


Fig. 5: General layout of the whole system

Measurement of electrical quantities were carried out using a multimeter. After carrying out the experimentation and testing the system, the efficiency of the solar panel, wind turbine and the inverter were then computed. The efficiency of the solar panel was determined using equation 3. The efficiency of the wind turbine was determined using equation 8. The efficiency of the inverter was determined using equation 14.

Results and Discussion

Figures 6 and 7 show the mean daily variation of solar insolation and wind speed during the period of the study. Figure 6 shows that the mean solar insolation during the period of February to April was fairly constant within the range of $400 \leq 200 \text{ W/m}^2$, with the distribution for February indicating some prominent peak values. This strengthens the viability of the results of the system's operation as the fairly steady insolation encourages smooth

power generation. Figure 7 shows a fairly similar variation of the mean wind speed as the insolation also showing that the daily wind speeds for February were higher for most of the days. Both of the parameters indicated reasonable fluctuations indicative of the effects of climate change. Apart from the fact that the mean wind speed for the period of the study falls below the wind speed range of 3 to 25 m/s for conventional wind turbine operation [50], the fluctuations strengthen the need for hybridization with solar energy in this case due to the abundance of the later resource in the location of the study [34, 48, 49]. However, the wind turbine in this study is a prototype with components well smaller than those of conventional turbines. With modern designs of wind turbines, the contribution of this resource could be better harnessed though it will raise the cost of the system.

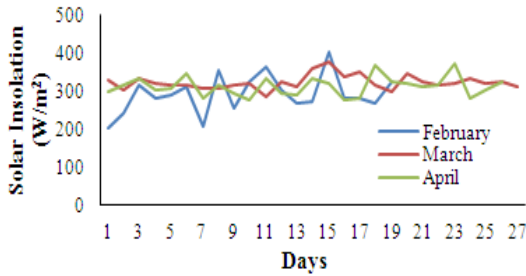


Fig. 6. Average Daily Solar insolation for the period of the study

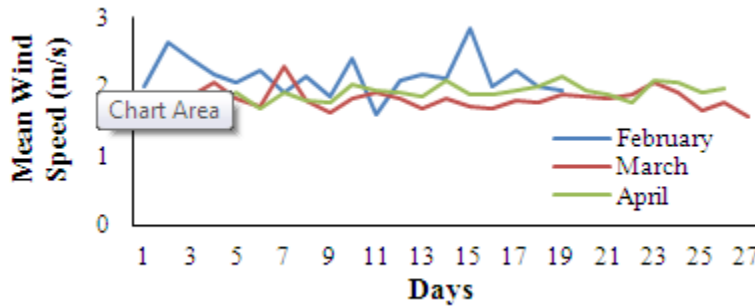


Fig. 7. Average Daily Wind Speeds for the period of the study

Table 2 shows the mean monthly solar insolation and wind speed for the period. It shows that high solar insolation does not necessarily translate to high wind speed. It also confirms the fact indicated in Figure 7 that the mean wind speed in February was the highest for the period.

Figure 8 shows the variation of voltage of the battery with the corresponding time of the day. It clearly shows the charging stages of the battery indicating the boost, floating and the trickle stages with the test period starting from 9 am to 4 pm. The Figure shows how the battery rapidly charged from 8.7 to 9.7 V within the hours of 9 am to 10 am thus indicating the boost stage (the initial charging state of the battery) as battery voltage increases. From 10 to 11 am, the battery voltage increased from 9.7 to 11.6 V indicating the floating stage. The trickle stage occurred within the peak periods of 12 to 4 pm leading to a gradual increase of battery voltage to 11.8 V and within this peak period there was high voltage demand from the users of these appliances in line with a study reported by [21] who carried out a work on the design and installation of a solar-wind hybrid power system to provide renewable electricity to a three-bedroom residential apartment in Ilaro Village of Ogun State. This signifies a favourable operation of the batteries [51].

Table 2. Monthly Average Solar Insolation and Wind Speed

Months	Average Solar Insolation	Average Wind Speed Value
--------	--------------------------	--------------------------

	(W/m ²)	(m/s)
February	277.3	2.15
March	323.6	1.82
April	312.7	1.9
Mean	304.5	1.96

Figure 9 shows the variation of the total load applied on the inverter with the number of hours used per day. It was observed that between the hours of 9 am to 12 pm, there was a low demand in the use of appliances as the time spent using the energy from the inverter increased. Within the hours of 1 to 3 p.m. there was a little drain of energy from the inverter and this was as a result of the high demand use of these basic appliances. These observations strongly agreed with the observations of [30] who designed and installed a solar-wind hybrid power system to provide electricity for a two-bedroom residential apartment in Ilorin, Kwara State, and [17] who provided energy supply to a two storey commercial building using solar-wind hybrid power system consisting of 6 kW solar panels, 2 kW wind turbine, 5 units of 24 V/600 Ah batteries and 6 kW inverter unit in Torankawa village in Sokoto state to meet its energy demands.

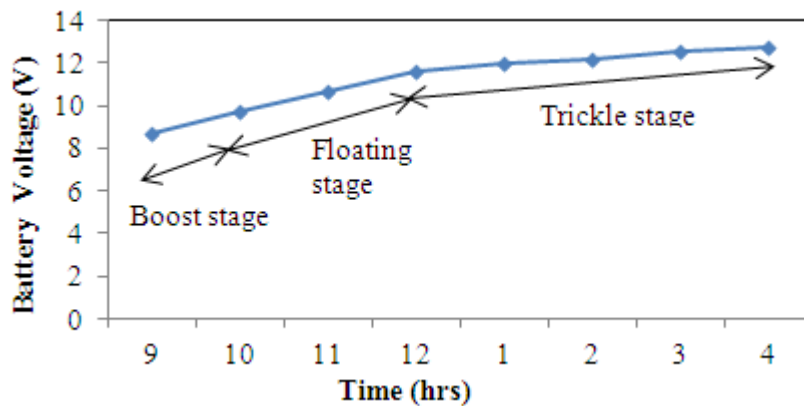


Fig. 8. Battery voltage against time

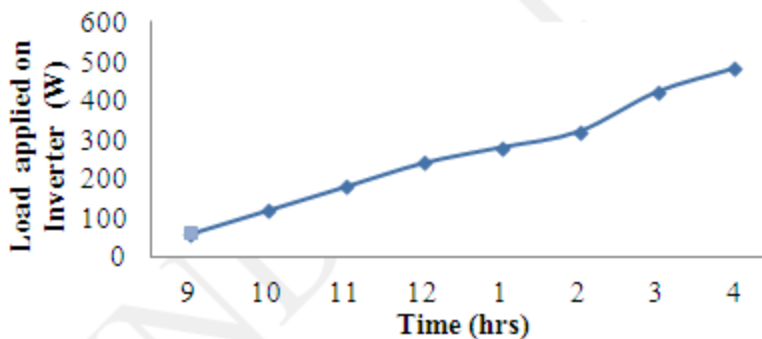


Fig. 9. Load applied on Inverter against hours used per day.

Figures 10 and 11 show that the off-load and on-load inverter DC voltages were fairly constant, indicating steady power generation during the period. There was hardly any difference between both voltages for February and April. However, the on-load voltages were higher in March than the ones for February and April and lower for the off-load. On the whole, the trends of the voltages portray good potentials for implementation of the system [52].

Figure 12 presents the cash flow summary and shows that in the optimized solar-wind hybrid power system configuration, the overall initial capital cost value required for investment into the system was \$683 (₦ 228, 805). The PV had the highest capital cost of \$282 (₦ 94, 470). Capital cost is the total cost needed to install the components at the beginning of the project implementation period [44].

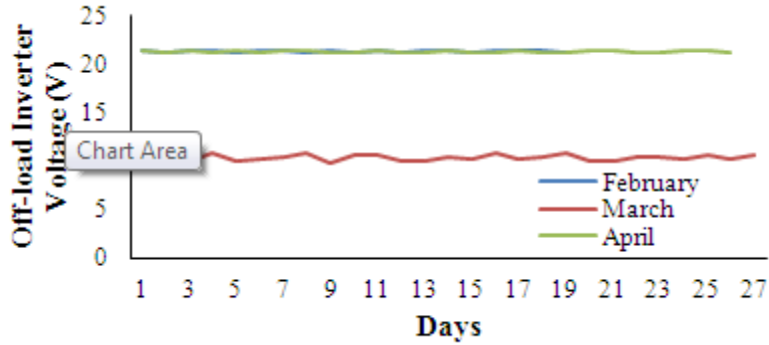


Fig. 10. Average Daily Off-load voltage on the Inverter for the period of the study

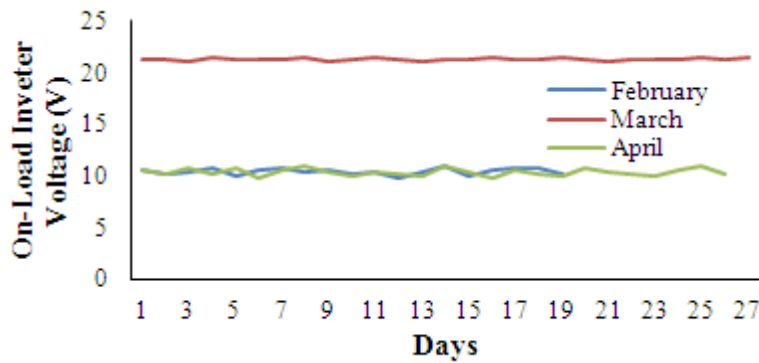


Fig. 11. Average Daily On-Load Voltage on the Inverter for the period of the study

The VLA6CRV220 battery had the second highest capital cost value of \$172 (₦ 57,620), the SPMG426C150 wind turbine had the third highest capital cost value of \$153 (₦ 51,225) and the inverter had the least capital cost value of \$76 (₦ 25,460). The reason for high capital investment into PV panels was due to the high availability of solar insolation in Makurdi which had led to the increase in the purchasing price of solar panels in the market. The low capital cost on the inverter was due to the materials used in fabricating the inverter such as integrated circuit, resistors, capacitors, light emitting diodes, lead connecting wires, etc. which were very much available in the market thereby making the inverter cheaper in terms of cost. This is the usual trend with renewable energy systems with reasonably very high initial costs [40].

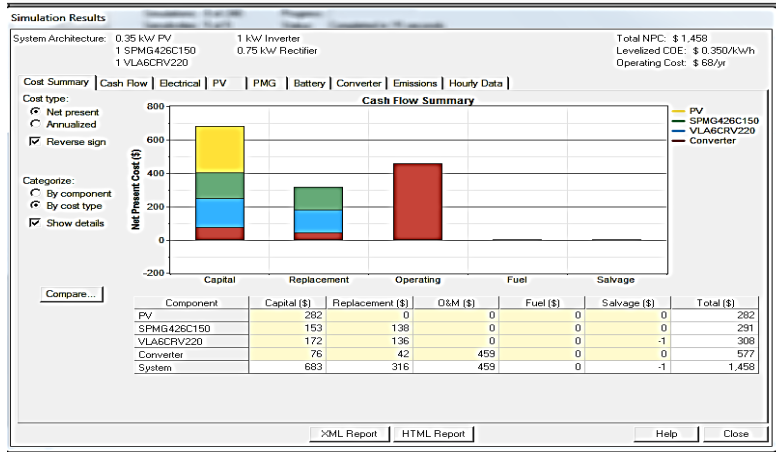


Fig. 12. Cash flow summary

Replacement cost is the cost value needed for replacing worn out components and this is quite different from capital cost because at the end of the lifetime of the components, only worn out parts will be due for replacement [15]. The SPMG426C150 wind turbine had the highest replacement cost value of \$138 (₦ 46, 230). This high replacement cost was as a result of the type of wind generator used. It was also observed that with time, the wind generator ought to be replaced for future effective use. The VLA6CRV220 battery had the second highest replacement cost value of \$136 (₦ 46, 230), the inverter the third highest replacement cost of \$42 (₦ 14, 070) while the PV had the least replacement cost of \$0. The reason for the \$0 cost value on the PV panel was that after the exhaustive life span of the PV, there is every tendency to buy a new panel as there was no need for it to be replaced again [39, 53]. Due to the functional use of the wind generator in converting the available wind speed into electrical energy from the turbine system to the inverter, it was observed that this component could be replaced as its functional use diminishes with time which may be the reason for its high replacement cost [13, 54].

Operations and maintenance cost is the sum of the annual cost which is needed for maintenance of the system components [43]. The inverter had the highest operation and maintenance cost of \$459 (₦ 153, 765) because the bulk of operation of the solar-wind hybrid power system depended solely on the inverter whose function is to switch from D.C to A.C. The PV panels, SPMG426C150 (wind turbine) and the VLA6CRV220 (battery) had operation and maintenance costs of \$0. The high operation and maintenance cost of the inverter was due to its excessive functional use in providing energy supply to the office.

From this system configuration no fuel consumption was recorded meaning that the cost of fuel was \$0 for PV, SPMG426C150 (wind turbine), VLA6CRV220 (battery) and inverter respectively. The main reason for the zero-dollar cost value on the components was due to non-use of diesel generator. This work strongly agreed with the observation of [22] who did an extensive work on the design and installation of a solar-wind hybrid power system for a 1 MW telecommunication base station in Etsako, Benin.

Salvage cost is the resale value of an asset at the end of its useful life. From Figure 9, the VLA6CRV220 (battery) was the only system component that had a salvage cost of \$1 (₦ 335) and this implies that after its useful life, the specified component under salvage value will be resold at a least cost. The PV, wind turbine and the inverter had no salvage cost after its useful life [54].

The levelized cost of energy is a critical value because it reflects how much the system is reliable and useful. HOMER does not rank systems based on cost of energy but based on its net present cost. In comparison to a work carried out by [15] on the optimal sizing of a solar-wind hybrid power system for distributed generation for utilization of resource available at Sagar, a remote off-grid island located in India in which simulation tests of different hybrid systems such as the solar-wind hybrid power system and the solar/wind/diesel hybrid system were carried out, the conclusion was that the solar-wind hybrid system will require less cost per unit of electricity in terms of net present cost. In contrast, [33] worked on the design and installation of a solar - wind hybrid power system to supply energy to a 3 storey commercial building in Ilorin, Kwara State, consisting of 9 kW PV panels, 10 kW wind turbine, 4 batteries of 24 V capacity and 5 kW inverter, and after successive simulation using HOMER, obtained a net present cost as \$12,884 (₦ 4,316,140) and levelized cost of energy as \$0.619 kWh. The reason for the net present cost and the cost of energy value being selected was due to its least cost for the above parameters and

HOMER categorized this as the best and efficient hybrid energy configuration after running and displaying series of categorized simulations [11, 22, 28].

Figure 13 shows the cash flows for the solar-wind hybrid power system. Cash flow clearly identifies how many years the investment will continue to support. It also determines how long the system is going to stand without any more investment on it and after how many years the user should invest again [42]. 20 years was chosen for this project because most of the designs of solar-wind hybrid power systems had their investment years fall within 20-25 years [55]. 20 years was chosen as how long the investment is expected continue to support. From the Figure, it was observed that the greatest contributor to the discounted cash flow was the PV panel which occurred on the 0th year, the VLA6CRV220 battery and the SPMG426C150 wind turbine had the second and third highest contributions to the discounted cash flow respectively at the initial year. Year 5 and 15 had a higher discounted cash flow contributed by the wind turbine followed by the inverter which contributed a little within the specified period except for year 10 in which the inverter contributed most to the discounted cash flow. The wind turbine contributed a little fraction to the discounted cash flow within this year. Year 7 and 14 had a higher discounted cash flow contributed by the battery while the inverter contributed little. Years 1 – 4, 6 – 9, 11 – 13, and 16 – 20 had the highest contributions to the discounted cash flow from the inverter respectively. These specified years were utilized by the inverter because of its functional use and this was the reason why more funds were channeled into the operation and maintenance of the inverter [56, 57].

Figure 14 shows the monthly average electric energy production from solar and wind energy. The yellow colour indicates electric energy production from solar energy while the green colour indicates that from wind energy. It was observed that the PV array contributed 98% (518 kWh/year) to electric energy production while the wind turbine system contributed 2% (10 kWh/year). Electricity produced by solar PV was considered as the base load of the solar-wind hybrid power system due to the favourably high insolation in Makurdi region and this gave a good possibility to engage the PV as a component of an integrated renewable power system to supply electricity to the departmental office at the location of the study. The wind speed in the location for the period of the study was relatively low with an average value of 1.96 m/s. From the monthly average electric energy production excess electricity, unmet electrical load, capacity shortage and renewable fraction were outputs results from HOMER [28, 50]. The monthly average electricity production had an excess electricity value of 140 kWh/year representing 26.6 % and this may have been as a result of the excess resource of solar which was above demand load and because the batteries were unable to store the produced electricity [40]. The excess electricity was fairly much because of the low load profile used in this study as compared to the much PV output due to high solar insolation. There was an unmet load of 1.56 kWh/year representing 0.4 % and a capacity shortage of 1.72 kWh/year representing 0.5%.

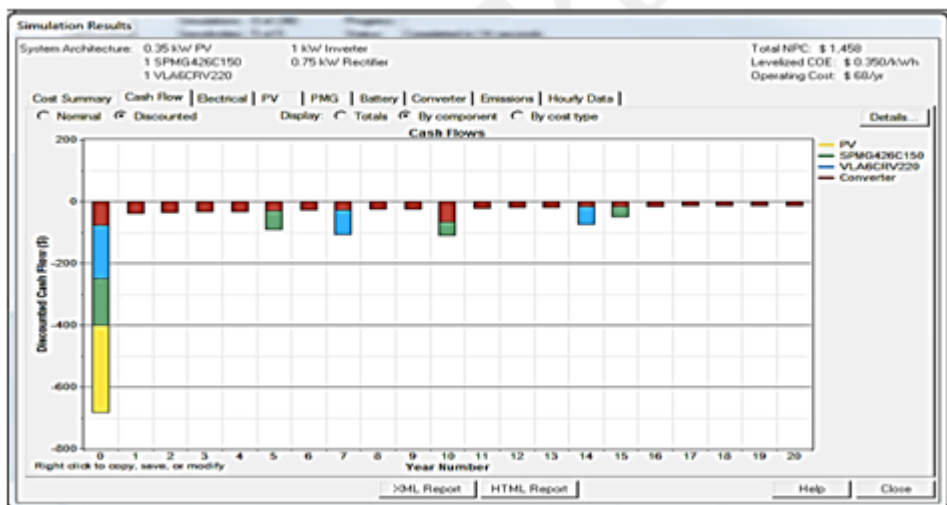


Fig. 13. Cash flows

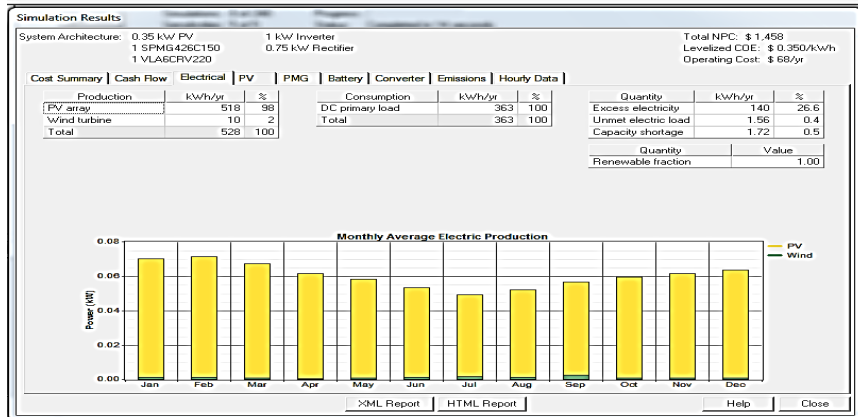


Fig. 14. Monthly average electric production

Figure 15 shows the simulation results obtained from the PV system and its D-map chart shows that the PV output fell within the range of 0.036 to 0.252 kW. The output features of the PV system included the rated capacity, mean output, capacity factor, total production, minimum output, maximum output, PV penetration, hours of operation and levelized cost. Rated capacity is the capacity rate of the PV array under standard conditions and the rated capacity value for this research was 0.350 kW. Capacity factor is the average power output of the PV array divided by its rated power in percentage and the capacity factor was 16.9 %. Total production is the total power output of the PV array over the period and its electric energy production output was 518 kWh/year. The minimum power output of the PV array over the period was 0.00 kW and this occurred when the panel did not get enough solar insolation to produce electricity. The maximum power output of the PV array over the period had a value of 0.34 kW. PV penetration is the average power output of the PV array divided by the average primary load in percentage. The PV penetration was 142 %. Hours of operation which was stated as the number of hours of the period during which the PV array output was greater than zero had its value as 4.48 h/year, levelized cost which is defined as the cost of energy of the PV array had a value of 0.0473 \$/kWh. These all indicate good potential for the system considering the capacity of the components selected for this prototype [58-60].

Figure 16 shows the simulation results obtained from the wind turbine. The output features of the wind turbine include the rated capacity, mean output, capacity factor, total production, minimum output, maximum output, wind penetration, hours of operation and levelized cost. Rated capacity which is the highest power amount from the wind turbine had a value of 0.1 kW. Mean output is the average power amount of the wind turbine over the period and its mean output value was 0.0 kW. Capacity factor is the average power output of the wind turbine divided by its rated power in percentage. Its capacity value was 1.15 %. Total production of the wind energy is the total power output of the wind turbine over the period, its total production output was 10.1 kWh/year, and maximum power output of the wind turbine over the period was 0.12 kW. Wind penetration which had a value of 2.75% is the average power output of the wind turbine divided by the average primary load, its wind penetration was quite low and this was due to the low average wind velocity of 1.96 m/s in Makurdi region at the period of study [24, 34, 50, 61].

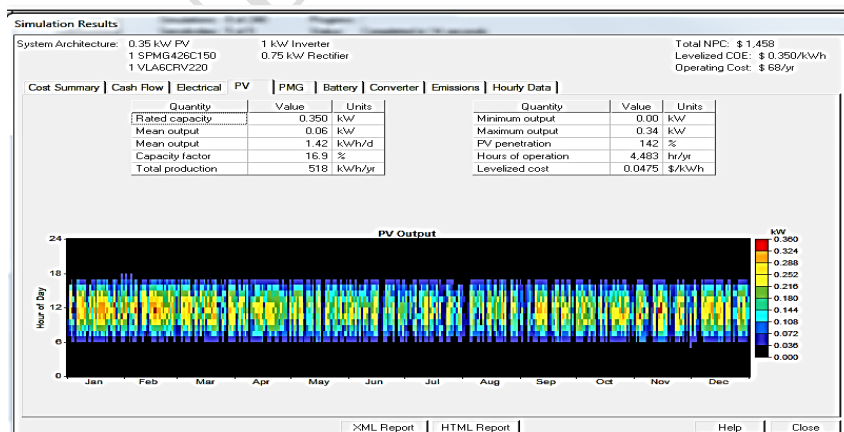


Fig. 15. Photovoltaic system simulation output

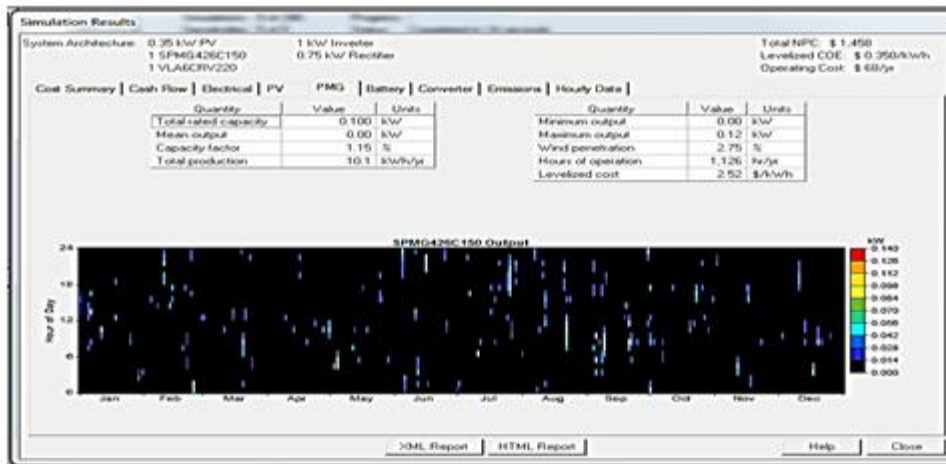


Fig. 16. Wind turbine simulation output

Levelized cost is the cost of energy of the wind turbine. Its levelized cost had a value of 2.52 \$/kWh, and this is in line with the work carried out by [4] on a PV-wind hybrid power system located in Zimbabwe region, which shows that the total production from wind (20.5 kWh/year) was relatively low when compared to PV which had a total production output of 1000 kWh/year, the maximum and minimum output were 12.1 kW and 1.2 kW respectively. Figure 17 displays the battery simulation results of the solar-wind hybrid power system and the frequency histogram from the chart displayed its initial state of charge from 30% and battery capacity of 12 V/200 Ah. The output features include nominal capacity, autonomy, lifetime throughput, battery wear cost, average energy cost, energy in, energy out, storage depletion, losses, annual throughput and expected life. Nominal capacity which is the amount of energy that could be withdrawn from the battery starting from the fully charged state had its nominal value as 2.40 kWh, usable nominal capacity is the battery capacity adjusted to exclude all capacity below the minimum state of charge of the battery and its was obtained as 1.68 kWh. The minimum state of charge is the state of charge below which the battery must not be discharged to avoid permanent damage. Its state of charge as indicated in Figure 14 was at 30 %. Autonomy is the capacity of the battery bank divided by the average electrical load, its value was 40.3 hours. Lifetime throughput is the total amount of energy that can be cycled through the battery before it needs to be replaced and this had a value 750 kWh. Battery wear cost is the cost of cycling energy through the battery bank, its value was 0.179 \$/kWh. Energy in is the total amount of energy charged to the battery with a value of 125 kWh/year. Energy out which is the total amount of energy discharged from the battery had a value of 100 kWh/year. Storage depletion which is the difference in the battery state of charge at the beginning and end of the period, has its storage depletion as 1 kWh/year. The results of the simulation indicate good promise for the implementation of the system and for its extension to supply a bigger power demand when scaled up and low wind speed turbines employed [32, 57, 62]. The observed result was in line with the work carried out by [47] on the design and installation of a solar-wind hybrid power system to supply energy for the Department of Physics, Sokoto State University. The system consisted of 1 kW PV panels, 300 W wind turbine, two deep cycle batteries (12 V/200 Ah) and 1600 W inverter. From the battery simulation results, the output features such as battery state of charge, autonomy, lifetime throughput, battery wear cost, energy in, energy out, storage depletion, losses, expected life and nominal value had its output values of 30 %, 40.8 h, 790 kWh, 0.179 \$/kWh, 129 kWh/year, 106 kWh/year, 1.6 kWh/year, 28 kWh/year, 7.20 year and 2.60 kWh respectively [47].

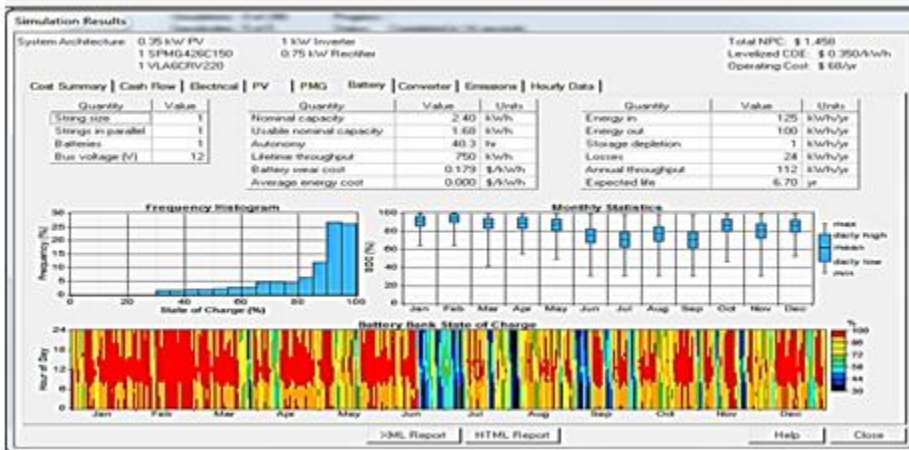


Fig. 17. Battery simulation output

Figure 18 shows the inverter simulation results. The output variables include capacity, mean output, capacity factor, hours of operation, energy in, energy out and losses. The inverter had an overall power rating of 1600 W. This described the power that would be available to the device in converting the D.C to A.C electricity. Wiring and heating losses were observed during the inverter operation. Usually, a suitable inverter for each installation can be selected based on the system capacity [7, 60, 63].

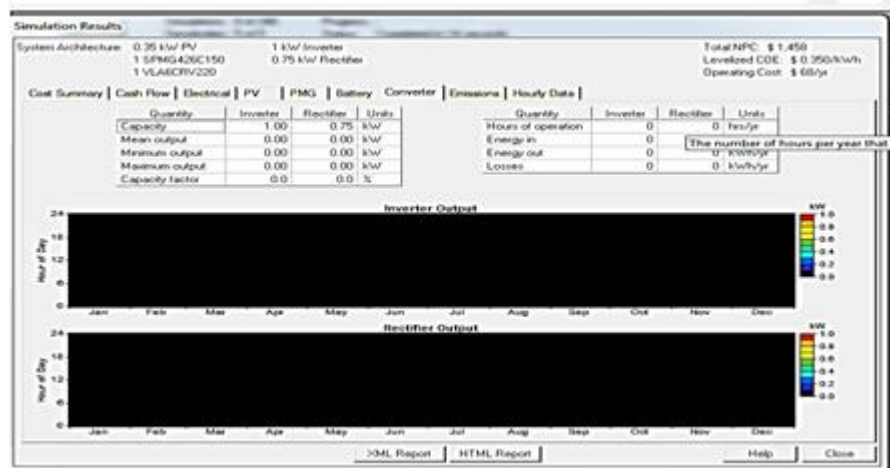


Fig. 18. Inverter simulation output

Figure 19 shows the gaseous emission level output. The emission of pollutants such as carbon dioxide, carbon monoxide, unburned hydrocarbons, particulate matter, sulphur dioxide and Nitrogen oxides had emission values of 0 kg/year respectively. The reason for this zero-emission value was due to non-use of a fossil fuel-fired generator in the solar-wind hybrid power system. The zero emissions of gases by the solar-wind hybrid power system clearly shows that the system was environmentally friendly [13, 64, 65]. Furthermore, the minimal noise pollution of the wind turbine and almost negligible hazard to birds largely attributed to the capacity of the system is a little added incentive [35, 66].

Table 3 presents the mean efficiency of the components. The efficiency of the wind turbine system and the solar panel were calculated as 48 % and 29.2% respectively. Considering that most solar panels are 11 % to 30 % efficient the solar panels used in this research were comparatively more efficient and the value of 29.2 % only represents the maximum efficiency under ideal conditions [67, 68]. However, it is important to consider that the actual efficiency

will depend on other factors such as the panel orientation, panel pitch, temperature and shade [41, 46, 69]. The efficiency of the inverter system was 50 % and its efficiency was determined from the average rate of off-load voltage to the on-load voltage. The inverter efficiency of 50 % was quite on the average when compared to other research work carried out by [3]. The low efficiency of the inverter could be as a result of the substantial presence of wiring losses which can easily be corrected in future fabrications.

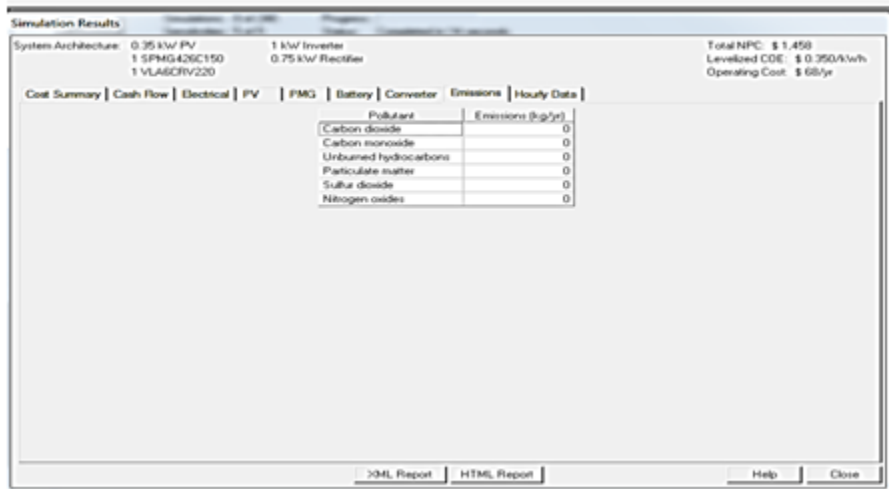


Fig. 19. Gaseous emission simulation output

Table 3. Components Efficiency

Component	Efficiency %
Wind Turbine System	48 %
Solar Panel	29.2%
Inverter	50%

CONCLUSION AND RECOMMENDATIONS

Following the observations from this work aimed at determining the feasibility of the solar-wind hybrid power system for implementation in the Mechanical Engineering departmental office at Joseph Sarwuan Tarka University, Makurdi, the optimized configuration of the system based on the net present cost, its levelized cost of energy, its renewable fraction and operating cost consists of 0.35 kW PV panel, 1 SPMG426C150 wind turbine (0.1 kW), 2 VLA6CRV220 battery and 1600 W inverter. The total net present cost of the system was \$1,458 (₦ 219,600.00), its levelized cost of energy 0.350 \$/kWh (₦70/kWh) its renewable fraction was 1 and its operating cost was \$ 68/year (₦ 13600.00/year). The efficiency of the wind turbine system, PV solar panels and the Inverter system were 48, 29.2 and 50 % respectively. The prototype of the solar-wind hybrid power system was able to meet the load demand of 425 W for the basic appliances considered in the office. Based on the results obtained, **it is hereby recommended that the system be implemented to examine the performance under actual working conditions of the office** and that the template be expanded to produce green energy for the entire University environment.

REFERENCES

1. Dunmade, I.S. (2017). Indicators of Sustainability: Assessing the Suitability of a Foreign Technology for a Developing Economy. *Technology in Society*, (4):461-471.
2. Tiller, C. (2017). A case study of a large scale solar and wind power hybrid system at Fakken Wind farm. Master thesis dissertation, the Arctic University of Norway, June 2017. Adejumobi, I. A., Oyagbinrin, S. G., Akinboro, F. G. and Olajide, M. B. (2011). Hybrid Solar and Wind Power: An Essential for Information Communication Technology Infrastructure and People in Rural Communities, (9)130-138.

3. Zhang, L., Gari, N. and Hmurcik, L. V. (2014). Energy Management in a Micro grid with Distributed Energy Resources. *Energy Conversion Management*, (78):297–305.
4. Arribas, L. (2009). PV-Wind Hybrid System Performance: A New Approach and a Case Study. *Renewable Energy*, (35):128-137.
5. Zohuri, B. (2018). Hybrid Energy Systems, 1-38, Springer International Publishing AG 2018. https://doi.org/10.1007/978-3-319-70721-1_1
6. Himanshu, S. (2017). A Control Strategy of Hybrid Solar Wind Energy Generation System. *Archives of Electrical Engineering*, (2):241-251.
7. Bizon, N., Oproescu, M. and Raceanu, M. (2018). Efficient Energy Control Strategies for a Standalone Renewable/Fuel Cell Hybrid Power Source. *Energy Conversion Management* (90):93–110.
8. Tascikaraoglu, A., Boynuegri, A. R. and Uzunoglu, M. (2014). A Demand Side Management Strategy Based on Forecasting of Residential Renewable Sources: A Smart Home System in Turkey. *Energy Build*, (80):309-20.
9. Shaffic, S., Nicholas, K. and Noble, B. (2020). Designing a Solar and Wind Hybrid System for small-scale irrigation: A Case Study for Kalangala District in Uganda. *Energy, Sustainability and Society*, (10):6.
10. Reddy, D.C (2018). Design of Hybrid solar wind energy system in a microgrid with MPPT Techniques, *International Journal of Electrical and Computer Engineering* (IJECE), 8(2): 730 – 740.
11. Hadi, N. A., Ateeb, H., Yuhani, P. W., Jubaer, A., Kamyar, M., San Chuin, L. And Zulkurnain, M. (2021). Sizing and Economic Analysis of Stand-Alone Hybrid Photovoltaic-Wind System for Rural Electrification: A Case Study Lundu, Sarawak. *Cleaner Engineering and Technology*, (4):100-191.
12. Weiping, Z., Akbar, M., Marc A. R. And Jingqing, L. (2019). Sizing a Stand-Alone Solar Wind-Hydrogen Energy System Using Weather Forecasting and a Hybrid Search Optimization Algorithm. *Energy Conversion and Management*, (180) 609–612.
13. Kavitha, S. (2013). Solar Wind Hydro Hybrid Energy System Simulation, *International Journal of soft computing and Engineering*, (6):28.
14. Sunanda, S. P. (2015). Prospects of Solar Photovoltaic Micro Wind based Hybrid Power Systems Western Himalayan State of Himachal Pradesh in India, *Energy Conversion and Management*, (105):1340 -1350.
15. Vikas, K. (2016). Solar-Wind Hybrid Renewable Energy system. A Review. *Renewable and Sustainable Energy Review*, (58):23-33.
16. Vivek, D. and Bhatia, J. S. (2013). Analysis and Design of a Domestic Solar-Wind Hybrid Energy System for Low Wind Speeds, *International Journal of Computer Applications*, (22): 234-245.
17. Zade, A.B (2016). Hybrid solar and wind power generation with grid interconnection system for improving power quality, power electronics, *intelligent control and energy systems* pp: 50 – 58.
18. Subodh, P., Shrestha, J. N., Fernando, J. N., Ferreira, J. A. F. and Muna, A. (2014). Optimization of Hybrid PV/Wind Power System for Remote Telecom Station. Conference Paper · December 2014 DOI: 10.1109/ICPES.2011.6156618.
19. Thakur, M. S., Gupta, B., Kumar, V., Pandey, M. (2012). Renewable Hybrid Energy System for Sustainable and Economical Power Supply- A Review, *International Journal of Engineering Research & Technology* (IJERT), Vol. 1 Issue 6, 1-9.
20. Thanh-Tuan, N. and Tobias, B. (2021). Multi objective Optimization of a Hybrid Wind/Solar Battery Energy System in the Arctic. *Journal of Renewable Energy* <https://Doi.Org/10.1155/2021/8829561>
21. Adejumbi, I. A., Oyagbinrin, S. G., Akinboro, F. G. and Olajide, M. B. (2011). Hybrid Solar and Wind Power: An Essential for Information Communication Technology Infrastructure and People in Rural Communities, (9)130-138.
22. Ajao, K. R., Oladosu, A. and Popoola, T. (2017). Using HOMER Power Optimization Software for Cost Benefit Analysis of Hybrid-Solar Power Generation Relative to Utility Cost in Nigeria. *IJRRAS*, (1)7.
23. Lakshmi, G., Rama Rao, P. V. V., Palleswari, Y. R. (2014). Hybrid solar-wind-hydro renewable energy system, *World Journal of Modelling and Simulation*, Vol. 10, No. 4, 243-251.
24. Marisarla, C.F and Kumar, K.R (2021). A Hybrid Wind and Solar Energy System with Battery Energy Storage for an Isolated System. *International Journal of Engineering and Innovative Technology*, (3):99-104.
25. Vincent, A. and Bahijahtu, A. (2014). Feasibility and Simulation of Integrated Renewable Energy System for Power Generation. A Hypothetical Study of Rural Health Clinic in Borno State.
26. Rohini, A. and Kord, H. (2015). Modeling of a Hybrid Power System for Economic Analysis and Environmental Impact in HOMER. *Proceedings of IEEE*, 11-13th May.
27. Tugnoli, A, Santarelli, F and Cozzani, V. (2016). An Approach to Quantitative Sustainability Assessment in the Early Stages of Process Design. *Environmental Science Technology*, (12):4555 – 4562.
28. Kanaska, A. A., Gajbhiye, V. K. and Jawore, S. J. (2019). Solar–Wind Hybrid System – A Review. *International Journal of Research in Advent Technology*, (5):2321 – 9637.

29. Ram, J.P (2017). Design and overview of maximum power point tracking techniques in wind and solar photovoltaic systems, a review “*Renewable and Sustainable energy reviews* 73: 1138 – 1159.
30. Robinson. (2016). Simulation and Evaluation of a Hybrid Concentrating Solar and Wind. *Renewable Energy*, (96):863-871.
31. Yashwant, S., Gupta S.C, Bohre A.K and Meny W. (2016). PV wind hybrid system: A review with case study. *Cogent Engineering* 3 (1), 1 – 31.
32. Kaldellis, J. K. (2020). Stand-alone and Hybrid Wind Energy Systems: Technology, Energy Storage and Applications. New York: Woodhead Publishing Limited.pp: 450 – 462
33. Mandell, J.F., Samborsky, D.D., Wang, L., and Wahl, N.K. (2017). New Fatigue Data for Wind Turbine Blade Materials,” *Journal of Solar Energy Engineering*, (125):506-514.
34. Lehtovaara, M., Karvonen, M., Kapoor, R., Sakari, T., and Pyrhönen, K. J. (2014). Major factors contributing to wind power diffusion. *Foresight*, 16(3), 250 - 269.
35. Clarke, S. (2018). Electricity Generation using Small Wind Turbines at Your Home or Farm, Ontario Ministry of Agriculture and Food, Fact Sheet in *Proceedings of International Conference* pp: 100 – 115.
36. Alghamdi FH. (2016). Wind Energy, International Journal of Scientific & Engineering Research, Volume 7, Issue 1, 65-79.
37. Kolhe, M., Agbosson, K. and Hamelin, J. (2015). Analytical Model for Predicting the Performance of Photovoltaic Array Coupled with a Wind Turbine in a Standalone Renewable Energy System Based on Hydrogen. *Renewable Energy*, (28):727-742.
38. Patel, R. M. (2006). Wind and Solar Power Systems: Design, Analysis, and Operation. United States: CRC Press Taylor and Francis Group.
39. Monaaf, D. (2017). A Review on Recent Size Optimization Methodologies for Standalone Solar and Wind Hybrid Renewable Energy System. *Energy Conversion and Management* 143: 252 – 274.
40. Dalwadi, P.G and Mehita, C.R (2017). Feasibility Study of Solar Wind Hybrid Power System, *International Journal of Energy Technology and Advanced Engineers*, (2):125-128.
41. Luque, A. and Hegedus, S. (2017). Handbook of Photovoltaic Science and Engineering. Second Edition. Chichester, West Sussex, and U.K: Wiley.
42. Markvart, T. and Castañer, L. (2020). Practical Handbook of Photovoltaic Fundamentals and Applications, Elsevier B.V. Oxford.
43. Barber, D. A (2016). Nigeria Moving into Solar Energy to Spur Business Growth. Accessed on 22nd March 2015 at <http://afkinsider.com/34905/nigeria-moving-solar-energy-spur-business-growth/>
44. Mbakwe, S. N., Iqbal, T. M. and Hsiao, A. (2018). Design of a 1.5 kW Hybrid Wind/Photovoltaic Power System for a Telecoms Base Station in Remote Locations of Benin City, Nigeria. necec.engr.ca/ocs2011/viewpaper.pdf.
45. Sinha, A.S (2019). Review of Recent Trends in Optimization for Solar- Photovoltaic Wind based Hybrid Energy System. *Review and Sustainable Energy Review*, pp: 50.
46. Yahia, B. (2016). Exploration of Optimal Design and Performance of Hybrid Wind-Solar Energy systems. *International Journal of Hydrogen Energy*, pp: 41.
47. Binayak, B. (2020). Optimization of Hybrid Renewable Energy Power Systems. *International Journal of Energy Engineering* (2): 99 – 112.
48. Antonio, J., C., Ange, O., and Costa, M. (2010). New procedure for wind farm maintenance. *Industrial Management & Data Systems*, 110(6), 861 - 882.
49. Kumar, A., and Nair, K. (2012). Wind characteristics and energy potentials at Wainiyaku Taveuni, Fiji. *Management of Environmental Quality: An International Journal*, 23(3), 300 - 308.
50. Li, G., Zhi, J. (2016). Chapter 2 - Analysis of Wind Power Characteristics, Editor(s): Ningbo Wang, Chongqing Kang, Dongming Ren, Large-Scale Wind Power Grid Integration, Academic Press, Pp. 19-51, ISBN 9780128498958, <https://doi.org/10.1016/B978-0-12-849895-8.00002-6>.
51. Ani, V.A., Nzeako, A. N. and Obianuko, J. C. (2018). Energy Optimization at **Data centres** in Two different Locations of Nigeria. *International Journal of Energy Engineering*, (4):151 –164.
52. Allan, R. S., Jose, M. C., Rodrigo, E. and Sergio, C. (2018). Multi-Objective Optimization Of Hybrid CSP/PV System Using Genetic Algorithm. *Energy*, (147):490-503.
53. Elhadidy, M. A. (2018). Opportunities for Utilization of Standalone Hybrid Power Systems in Hot Climates. *Renewable Energy*, (28):1741-1753.
54. Malysz, P., Sirouspour, S and Emadi, A. (2020). An Optimal Energy Storage Control Strategy for Grid-Connected Micro-Grids. *IEEE Trans Smart Grid*, (4):1785–96.

55. Mokhtara, C., Negrou, B., Settou, N., Gouareh1, A., Settou1, B. and Chetouane, M. A. (2020). Decision-Making and Optimal Design of Off-Grid Hybrid Renewable Energy System for Electrification of Mobile Buildings in Algeria: Case Study of Drilling Camps in Adrar. *Algerian Journal of Environmental Science and Technology*, (6)2.
56. Rajoriya, A. and Fernandez, E. (2018). Sustainable Energy Generation Using Hybrid Energy System for Remote Hilly Rural Area in India. *International Journal of Sustainable Engineering*, (3):219-227.
57. Jahanbani, F. and Riahy, H. (2018). Optimal Design of a Hybrid Renewable Energy Systems. *Renewable Energy Trends and Applications*, pp: 230-250.
58. Saidi, A and Chellali B (2017). Simulation and control of solar wind hybrid renewable power system and control (ICSC) 2017, 6TH International Conference on IEEE.
59. Villalva, M.G. (2009). Comprehensive Approach to Modeling and Simulation of Photovoltaic Arrays, *IEEE Transactions on Power Electronics*, (25):1198-1208.
60. Bekele, G. and Tadesse, G. (2014). Feasibility Study of Small Hydro/PV/Wind Hybrid System for Off Grid Rural Electrification in Ethiopia. *Applied Energy*, (65): 195 – 206.
61. Behnke, R., Member, S., Benavides, C., Lanas, F., Severino, B., Reyes, L., et al. (2017). A Microgrid Energy Management System Based on the Rolling Horizon Strategy. *IEEE Trans Smart Grid*, (2):996–1006.
62. Irwan, Y. M. (2017). A New Technique of Photovoltaic Wind Hybrid Power System in Perlis, Energy Procedia, *International Journal of Engineering and Advanced Technology* pp: 36- 44.
63. Chouaib, A., Djamel, B., Batoul, T. and Salim, M. (2021). Sizing, Optimization, Control and Energy Management of Hybrid Renewable Energy System-A Review. *Energy and Built Environment*, (23)53.
64. Anayochukwu, E. A. and Nnene, E.V. (2016). Simulation and Optimization of Hybrid Diesel Power Generation system for GSM Base Station Site in Nigeria. *Electric Journal of Energy and Environment*, (1)1.
65. Ghosh, T. and Prelas, M.A. (2013). Energy Resources and Systems. *Renewable Resources*, (2): 2011 Edition. Springer.
66. Ekpenyong, E.E, Bam, M.E and Anyasi, F.I (2015). Performance Analysis of an Installed 1.5 kVA Hybrid Power Supply. *Journal of Electrical and Electronics Engineering*, (3): 20 – 27.
67. Lazarov, V. D. and Hankins. F. (2017). Hybrid Power Systems with Renewable Energy Sources, Types, Structures, Trends for Research and Development in: *Proceedings of International Conference ELMA*. pp: 515–520.
68. Mustafa, E. and Dilşad, E. (2013). Sizing PV-Wind Hybrid Energy System for Lighting. *International Journal of Development and Sustainability*, (1):85-98.
69. Vincent, A. and Nzeako, A. (2012). Energy Optimization at GSM Base Station Sites Located in Rural Areas. *International Journal of Energy Optimization and Engineering* (IJE OE) 4th Edition, pp; 200 - 210.